Leakage Current and Pollutant Properties of Porcelain Insulators from the Geothermal Area

Waluyo [1], **Ngapuli Irmea Sinisuka**[2],
Suwarno [3], and **Maman Abdurahman Djauhari** [4], Non-members

ABSTRACT

This manuscript presents the experimental results of a new-clean and seven geothermal naturally polluted outdoor porcelain insulators. These insulators were tested in a hermetically sealed chamber, where their leakage currents and applied voltages were measured with a storage digital oscilloscope. The measured data could be recorded oscilloscope and transferred to a computer, saved in softcopy forms. FFT was used to analyze the leakage current waveforms, and correlation coefficient matrix and principal component analysis (PCA) were used to analyze the relation among parameters. It was also carried out EDAX tests of insulator adhered pollutant.

The results indicated that the power factors and leakage current amplitudes closed to humidity, the phase angle closed to THD, and temperature opposited the humidity. The ratios of insulator impedance on the high and low humidity were ranged from 0.8696 until 0.1343. The small insulator impedance ratios were rearched on the first and seventh withdrawals, i.e. 0.1363 and 0.1343 respectively. On these insulators, THD ratios on the same conditions were 0.3739 and 0.4598 respectively. These phenomena were caused by dry season, which amount of pollutant stuck on the insulator surfaces significantly. On the high humidity, the minimum phase angles ranged between 66.8 and 25.7 degrees. Sulfur chemical element was found in medium composition on the pollutant.

Keywords: Geothermal, Humidity, Leakage Current, Pollutant, Porcelain Insulator

1. INTRODUCTION

Overhead transmission or distribution lines are widely used in present power system to transmit electric power from generation stations to customer points. Their proper function depends on the insulation system with the supporting structures largely [1]. The performance of outdoor insulators, as main insulating material, is influenced by some parameters. Two of these parameters are environmental pollution and humidity.

Those lines sometimes traverse on many polluted or emitted areas, such as coastal, industrial and even geothermal areas. In a particular case of geothermal areas, transmission lines are used to transmit electric energy from a geothermal power plant to a switchyard of distribution.

Geothermal power stations create emission as chemical materials. Most chemical compounds are gas forms, especially CO_2 and H_2S. CO_2 is the major component (94-98%), H2S is around 1% and mercury concentration is only 1-10 mg/Nm3. Typical concentrations of mercury and hydrogen sulfide were the order of 10-20 ng/m^3 and 20-40 μg/m^3 respectively [2]. Geothermal fluids (steam or hot water) usually contain gasses, such as CO_2, H_2S, NH_3, CH_4, and trace amounts of other gases, as well as dissolved chemicals whose concentrations usually increase with temperature. For examples, sodium chloride (NaCl), boron (B), arsenic (As) and mercury (Hg) are source of pollution if discharged into the environment [3]. The typical non-condensable gasses (NCG) were contained in the steam flashed off the geothermal fluid from Icelandic high-enthalpy reservoirs were SiO_2, Na, K, Mg, Ca, Cl, SO_4 and Fe [4]. H_2S can reach moderate concentrations. The incineration process burns the gas from steam to convert H_2S to SO_2, the gases are absorbed in water to form SO_3 and SO_4 in solution. H_2S, HCl and CO_2 are undertaken [5]. As and Hg occur in geothermal waters. Hg occurs in geothermal systems due to the absorption of vapor and volcanic gasses into thermal waters. As and Hg dissolve in thermal fluids and concentrate in surface alterations. Chemical compositions of thermal waters are Cl, SO_4 and HCO_3 [6]. A gas stream containing H_2S can be converted into commercially quality sulfuric acid [7]. The incineration process burns the gas removed from the steam to convert H_2S to SO_2, absorbed in water to form ${SO_3}^{2-}$ and ${SO_4}^{2-}$ [8]. Major element compositions hot pools, geysers and cold

Manuscript received on July 31, 2009 ; revised on October 14, 2010.

This original work has been presented on ECTI-CON 2009, held at Ambassador City Hotel, Pattaya, Thailand on May 6-8th, 2009.

[2,3] The authors are with The Academic Staff, School of EE and Informatics, Bandung Institute of Technology, Indonesia , E-mail:ngapuli@hv.ee.itb.ac.id and suwarno@ieee.org

[4] The author is with The Academic staff, Faculty of Mathematics and Natural Sciences, Bandung Institute of Technology, Indonesia, E-mail:maman@math.itb.ac.idAlamat

meteoric waters at El Tatio were Ca^{2+}, Na^{+}, Mg^{2+}, K^{+}, Cl^{-}, tAlk, $SO_4{}^{2-}$, SiO_2. Otherwise, minor and trace element composition ones were Al, As, B, Ba, Br, Co, Cr, Cs, Cu, Fe, I, Li, Mn, Mo, Ni, Rb, Sr, Tl and Zn [9]. Typical geothermal fluids, with local shallow ground waters, were characterized by a relatively high concentration of K, Ca, NO_3, SO_4, and Cl [10]. The waters are mostly acid with pH between 1.5 and 7.9 caused by elevated SO_4 between 10 and 5066 ppm and are elevated in most metals including Fe (0.05-753 ppm) and Al (0.03-390 ppm) but low in Cl (1.4-17.9 ppm) [11]. H_2S from the steam is oxidized by the dissolved oxygen to form elemental sulfur or sulfuric acid (H_2SO_4) which lowers the pH value [12]. The gas exhausted from the O take geothermal power station is supplied to a specific hot solution in which a thermophilic sulfur oxidizing bacterium is cultured. In this solution, the bacterium converts H2S in the gases into H_2SO_4 [13]. Mercury levels in lichens were within the background range (0.1-0.2 microg/g dw). On the contrary, at Aiole, Hg concentrations (0.63-0.67 microg/g dw) were much higher than background. After the new geothermal power plant went into operation at Bagnore, lichen concentrations of Hg showed a 50% increase from 0.22 to 0.32 microg/g dw [14]. Boron removal after single stage regeneration with 10% H_2SO_4 was found to be possible [15]. NCG consist mainly of CO_2 and NH3 (97-99%) [16]. H2S content in NCG was 100-200 ppm [17]. Geothermal power plants (GTPP) could release from the non-condensable fraction of the steam: CO_2 (98%), H_2S (1.5%), methane (0.4%), hydrogen (0.1%). The oxidation of H_2S to SO_2 and its subsequent reaction to sulphate ions within the atmospheric produces aerosols representing a major component of acid rain. GTPP could also release, from the non-condensable fraction of the steams, trace amounts (0.001%) of ammonia, radon, boron, arsenic, cadmium and antimony. Ammonia and mercury may also enter local waters from geothermal steam condensation [18].

As scientific hypothesis, based on above cited references, those chemical compounds or elements, in a certain level, might reduce outdoor insulator performance. However, until now, it was still rare a research that consider an influence of geothermal area to outdoor insulator performance. Therefore, it was important to carry out a research concerning this condition.

The objectives of research were to obtain the tendency of leakage current properties on the porcelain insulators from the new clean to more than two years polluted conditions, which installed on the geothermal power plant area. The considered properties of leakage currents were their amplitudes, waveforms and phase angles. The harmonics and THD (total harmonic distortion) were the representation of waveforms. The relation among leakage current properties to environmental parameters were analysed by using correlation coefficient and principal component analyses, so that it could be understood the variables influence to each other. The major chemical elements of scraped pollutant were shown by EDAX (Energy Dispersive Analysis of X-rays) tests.

2. EXPERIMENTAL AND ANALYSIS METHODS

There have been many methods to measure leakage currents of outdoor insulators for research. The method of leakage current measurement in [19,20] used oscilloscope, computer and humidifier. Nevertheless, no applied voltage waveforms were shown. Other experiments were also shown leakage current waveforms [1,21-22]. Another method similar with [19] was in [23], but different in dimension. It was shown a nozzle facility on the chamber [24], and water steam to control humidity levels [25]. According to [26], the leakage currents were measured their rms values, instead of waveforms. An experiment with pressure under normal condition was also carried out on [27-29]. It was shown minimum AC flashover voltages. There was a measurement of leakage current and applied voltage simultaneously [30]. It was shown V-I characteristics theoretically [31].

In these measurements of research, it had some advance. The measurements of leakage currents were carried out from a new and clean until seven polluted identical 20 kV outdoor porcelain insulators gradually. The polluted insulators have been installed at PLN switchyard of Kamojang geothermal power plant, West Java, around 1447 m above sea level, on December 14^{th}, 2006 together, and then taken gradually around 3 to 4 months. These samples were made as close as possible to the geothermal power plant, only around 30 m, in order to be as representative as possible to the geothermal power plant condition. The samples were installed here to avoid disturbance from human kinds, including stolen. Only the authorized people could enter the switchyard.

After installation on the site, gradually they were taken to be tested at the laboratory. The insulator leakage currents were measured in a hermetically sealed chamber. The size of chamber was 120 cm × 150 cm × 120 cm (WxHxD). Researchers could adjust the temperature, humidity and pressure inside the chamber and the applied voltage of insulators simultaneously.

The temperature could be regulated by two elements of heater, for raising of temperature. This temperature was monitored by a high precision digital temperature indicator, where its sensor was PT100. Otherwise, the relative humidity inside chamber could be regulated by water steam which flowed to the chamber through a flexible pipe for raising humidity. In the chamber, it was put some amount of silica gel to fast reducing of humidity. This humidity

was monitored by a relative humidity (RH) indicator. Finally, the air pressure inside the chamber could be controlled by a vacuum pump and a compressor. The air pressure could be adjusted as positive or negative values, and could be monitored by a suitable high precision digital manometer. The digital manometer could monitor and display both positive and negative values of pressure.

The measurements of leakage current and applied high voltage waveforms used a two-channel storage digital oscilloscope. The leakage current signals were entered into the first channel, and the applied high voltage signals were entered into the second channel of the digital storage oscilloscope. The measured data could be recorded and transferred to a computer using USB and could be saved in softcopy form. Figure 1 shows the schematic diagram of experimental set up.

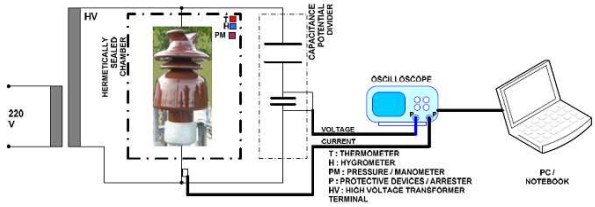

Fig.1: *Schematic diagram of experimental set up*

The applied high voltage magnitudes could be controlled by a regulator of the input or low voltage side of high voltage step-up transformer. Physically, the necessary main tools are shown by Figure 2.

Fig.2: *Main experimental equipments*

The main important tools for leakage current measurements were high voltage equipment (step-up high voltage transformer, resistor, power cable and capacitive voltage divider), a hermetically sealed chamber including controlling and monitoring devices (heater, water evaporator, vacuum pump, compressor, temperature indicator, RH indicator, positive-negative indicator manometer), the insulators as equipment under tests, a two channel storage digital oscilloscope, computer and necessary software. For pollutant test, it was used EDAX instrument.

This work was the concerning measurement of very small leakage current signals, which might be interfered by noise. The noise could not be omitted totally or perfectly. Nevertheless, this could be reduced as small as possible. The noise reduction could be carried out by some ways. The data cables, namely the cables for measurement of applied voltage from voltage divider output to the second channel of oscilloscope, and the cables for measurement of leakage current from the series resistor of low voltage or ground part of insulator under test to the first channel of oscilloscope, were coaxial type cables. The ground parts of cables were outer part conductor, and the live parts, which brought the measured voltage and leakage current signals, were inner or central part of cable conductors. Thus, the signals were hoped to be protected by ground parts of outer conductor from unnecessary noise. The outer part conductors were grounded. The signal cables were made as short as possible, as straight as possible and avoided unnecessary looping. Finally, the cable connections were clamped or soldered tightly. Based on these treatments, the unnecessary noise could be minimized.

After measurements of leakage currents, it was obtained numerical data 2500 points for every measurement. The real leakage current magnitudes were the measurement results which divided by the series resistor value. Whereas, the real applied voltage magnitudes were the measurement results which multiplied by the voltage divider constant. Furthermore the data of leakage current waveforms were analyzed by using fast Fourier transform. These implementations used the Danielson-Lanczos method [32]. Thus, the frequency spectra of leakage current waveforms could be obtained on the subjected insulators. Furthermore, we calculated the total harmonic distortion (THD). THD is defined as the total ratio of the harmonic components, except the fundamental, to the fundamental [33], as

$$THD = \frac{\sqrt{\sum_{n=2}^{\sim} I_n^2}}{I_1} \qquad (1)$$

Where I_1 is the harmonics amplitudes of fundamental frequency, and I_n are the n^{th} harmonics amplitudes of remaining frequencies.

The relations among parameters, either leakage current and environmental parameters or themselves,

were analyzed by using correlation coefficient analysis. A correlation coefficient matrix is derivation of covariance matrix to understand how much level of correlation among parameters base on data. A covariance value is defined by a formula as [34-35]

$$COV(X,Y) = \frac{1}{n}\sum_{j=1}^{n}(x_j - \mu_x)(y_j - \mu_y) \quad (2)$$

Where n is number of data, x_j and y_j are values of data on one and another variables, and μ_x and μ_y are corresponding mean of data for one and another variables respectively.
Furthermore, the components of coefficient correlation matrix is defined as :

$$\rho_{x,y} = \frac{COV(X,Y)}{\sigma_x \cdot \sigma_y} \quad (3)$$

Where σ_x and σ_y are variances of data on one and another corresponding variables.

The values of coefficient correlation components are between -1 until 1. If a value close to -1, it represents that one parameter highly influences to another, but it is reciprocal property. Otherwise, if a value close to 1, it represents that one parameter highly influences to another, in proportional property. Finally, if a value closes to zero, it is minor in dependency.

Besides using coefficient correlation matrix, it was also analyzed by using principal component analysis (PCA). PCA shows a scatter plot, which nearness among variables indicate the correlation level one to another variables. If a set of data is presented in matrix X, which X consists of some variables and a number of data, the main algorithm of PCA involves some steps [36-38].

Firstly, determine the mean components of matrix X, those related by

$$\bar{x}_l = \frac{1}{n}\sum_{k=1}^{n} x_{1,k} \quad (4)$$

Furthermore, determine covariance matrix using equation of

$$C = X * X^T \quad (5)$$

Finally, determine eigen values and eigen vectors of covariance matrix using the equation of

$$CQ = \lambda Q \quad (6)$$

Where λ are eigen values and Q are eigen vectors. Base on the eigen values, it is plotted their scatters in two dimensions, where the horizontal axis is first principal component and the vertical axis is second principal component. Finally, the nearness of parameters those plotted on PCA indicates the correlation level among parameters.

We used PCA, as part of multivariate statistical tool. Using this PCA, we can see which parameter influence dominantly each other. PCA describes correlations among parameters or variables statistically base on data. The data can not illustrate the correlations among parameters exactly in 100%. Nevertheless, PCA describes correlations among parameters in majority. By PCA, it is shown the closeness of parameters each other. If two parameters are very close, the first parameter influences significant proportionally to another one. If two parameters are in opposition very far, the first parameter influences significant reciprocally to another one. If two parameters are far in a same quadrant, it is minor dependency each other. Finally, if a parameter is close to central point of coordinate, it is minor to influence another one.

In this experimental research, it was not only on a value of temperature, humidity or pressure, but also on the various parameters for measuring the leakage currents. It was emphasized the **behavior** of leakage currents, which in this case represented by the amplitudes, phase angles and patterns of leakage currents on various conditions. A phase angle was the difference of the angle between leakage current wave and applied voltage wave. On an insulator, the phase angle is usually leading, due to capacitive property. Nevertheless, its value can change due to some factors. The patterns of leakage currents were represented by the amplitudes of leakage current harmonics and THD. Thus, it could be concluded which parameter was the most dominant to influence the leakage current. It was represented the actual conditions, especially relative humidity and temperature, on the site which had variation. It was more representative than that only one condition. Therefore, it was agree among the physical facility of experiments, multivariate statistical tool to analyze the data and a part of actual conditions on site.

Based on the coefficient correlation matrix and principal component analysis, the experimental results were analyzed and discussed the relation with the physical condition.

3. RESULTS AND DISCUSSION

3.1 The New-Clean Insulator

Actually there were many data of measurements. However, in this manuscript, it is presented two significant conditions, low and high relative humidity, on the new-clean and polluted insulators. Nevertheless, due to similar leakage current waveforms on polluted low humidity of insulators with that on the new-clean low humidity of insulator, so that it is revealed on high humidity only. Figure 3 shows the leakage cur-

rent and applied voltage waveforms of new-clean insulator on the conditions of 67%, 26.7 centigrade, -0.8 kPa and 9.24 kV for relative humidity, temperature, pressure and applied voltage amplitude respectively, as sample of low humidity.

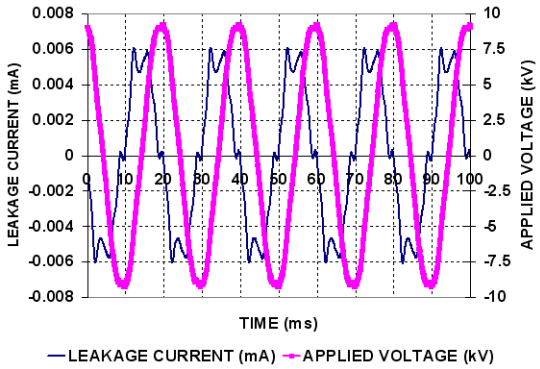

Fig.3: *The applied voltage and leakage current waves of low humidity new clean porcelain insulator*

On this condition, the phase angle was 81.3 degree, which meant the insulator, in new, clean and low humidity conditions, was very capacitive.

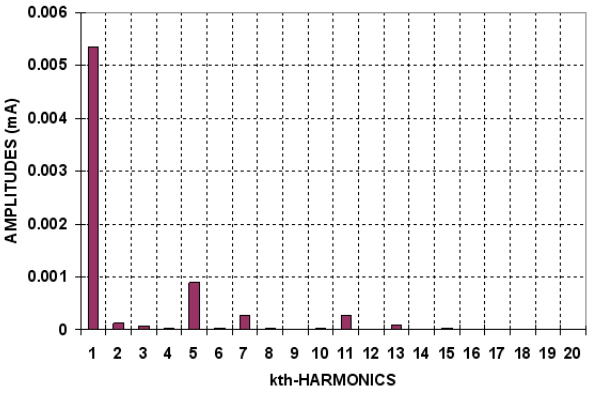

Fig.4: *The frequency spectrum of leakage current of the low humidity new-clean porcelain insulator*

Figure 4 shows the frequency spectrum of the leakage current waveform as shown by Figure 3. In this condition, the first to thirteenth odd harmonics were 87.87%, 1.28%, 14.93%, 4.26%, 0.19%, 4.87% and 1.13% respectively, compared to the leakage current amplitude, and THD was 18.6%. It was indicated that the second highest amplitude was fifth harmonics significantly, after the fundamental. THD was significantly high too. Whereas Figure 5 shows the leakage current and applied voltage waveforms of new clean insulator on 99% RH, 26.7 centigrade of temperature, without pressure and 8.6 kV maximum applied voltage conditions, as typical of high humidity condition.

From Figure 5, it is shown that the leakage current waveform on high humidity was different from the previous low humidity new-clean condition. The peak

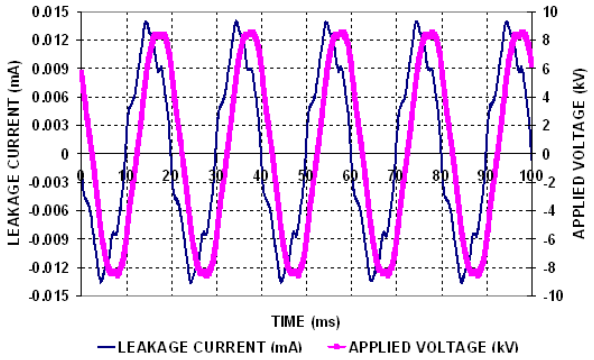

Fig.5: *The applied voltage and leakage current waveforms of high RH new-clean insulator*

forms of wave became sharper. This indication tent to approach a pure sinusoidal wave relatively rather than low humidity one. Otherwise, the phase angle was 46.7 degree and the amplitude of leakage current wave became higher than the low humidity previous condition. This phenomenon was dominantly caused by the water droplets spread out on the insulator surface. Therefore, the high RH made the new-clean porcelain insulator became little more conductive, rather than that low humidity condition. Nevertheless, the leakage current wave was not until pure sinusoidal wave, and the wave did not coincide to the applied voltage wave.

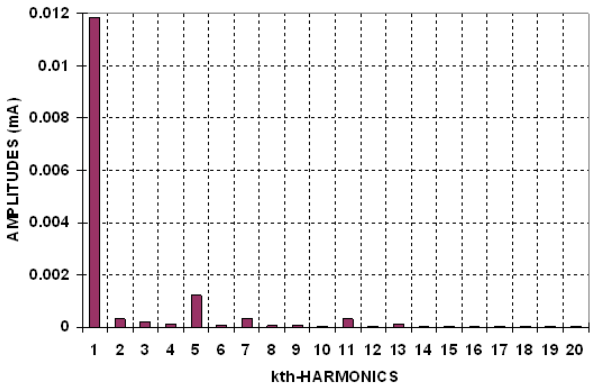

Fig.6: *The frequency spectrum of leakage current waveforms of high RH new clean porcelain insulator*

Figure 6 shows the frequency spectrum harmonics of leakage current waveform as shown by Figure 5. On this condition, the first to thirteenth odd harmonics were 85.8%, 1.43%, 8.84%, 2.39%, 0.43%, 2.26% and 0.89% respectively compared to the amplitude of leakage current wave. Whereas, the THD was 11.2%. It indicated that the amplitude percentage of fifth harmonics was lower than that on low humidity. The leakage current wave tent to close pure sinusoidal wave compared to the previous condition. This condition was also indicated by THD which lower that on low humidity. Nevertheless, this still worked nor-

mally.

Table 1 shows the correlation coefficients among parameters of new-clean porcelain insulator based on 82 data of leakage current measurement with various temperature, humidity, pressure and applied voltage amplitude. It is shown that the correlation coefficient between H (relative humidity) and I_{max} (leakage current amplitude) was high enough, as 0.56. The humidity influenced the leakage current amplitude significantly. The leakage current amplitude (LC) would increase if the humidity rose. Of course, the leakage current amplitude was highly influenced by applied voltage magnitude, that indicated by correlation coefficient of 0.73. The leakage current amplitude was proportional to most of harmonic amplitudes. The humidity influenced the phase angle and total harmonic distortion (THD) reciprocally and very significantly, where the correlation coefficients were -0.88 and 0.83 respectively. If the relative humidity rose, the phase angle would highly reduce. This meant that the power factor increased, which indicated by the correlation coefficient of 0.87. Otherwise, if the humidity increased, the THD would reduce significantly, which meant the leakage current waveforms tent to be more pure sinusoidal relatively, rather than that on the low humidity.

Otherwise, the correlations among parameters are shown by the principal component analysis on Figure 7. In this figure, it is shown that THD and PHA (phase angle) are close to each other, and opposition with H (relative humidity). This meant if the relative humidity increased, the phase angle and THD would reduce. Consequently, the increment of humidity would increase power factor (COS_PHA) of insulator. This is shown by H which very close to COS_PHA, and also it is indicated by the correlation coefficient of 0.87 on Table 1. Thus, in this condition, the influence of humidity was very significant to the insulator power factor or phase angle. Consequently, THD would reduce as relative humidity increased. This meant if the humidity rose, the leakage current waveform would tend to approach sinusoidal form relatively. Relative humidity (H) is shown as fairly opposition to temperature (T). This meant, if the temperature increased, the humidity would reduce considerably.

Other influence, if the humidity rose, the leakage current amplitude would increase slightly. This is indicated by leakage current amplitude (Imax) which relatively closes to humidity (H) on PCA. The consequence of leakage current rise was especially the amplitude of first, third, fifth and seventh harmonics also increased. Finally, pressure (P) is close to the central of PCA coordinate. This meant that the pressure did not influence other parameters practically. This was also supported by the correlation coefficient values of pressure, on Table 1, to other parameters were very small, approach to zero, far under absolute of 0.50.

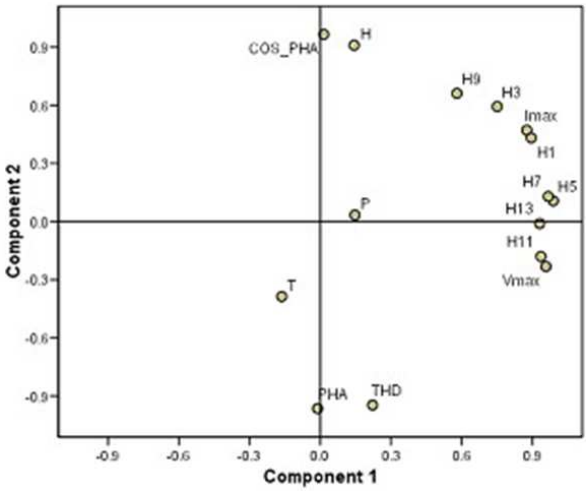

Fig. 7: *PCA of new-clean porcelain insulator leakage current measurement results*

3.2 The First Withdrawal Polluted Insulator

The polluted insulators were first to seventh withdrawals after polluted on the site of geothermal are. In general, on dry conditions, the waveforms and other behavior were similar. However, on high relative humidity, they were significantly different. Thus, it is presented the waveforms on high humidity only.

On the first removal porcelain insulator, which was withdrawn on August 31^{st}, 2007, the waveforms are shown by Figure 8. This condition was on 90% RH. 34.5°C, 42 kV_{max} and without pressure. The odd harmonics were 91.4%, 0.4%, 7.3%, 1.6%, 0.2%, 0.1% and 0.1% of leakage current amplitude, 206 μA. Otherwise, the impedance, THD and phase angle were 203 883 495 Ω, 8.26% and 35.6° respectively. It is shown that the leakage current waveform was more pure sinusoidal than that on dry condition, which similar with Figure 3. The leakage current amplitude was higher than that on low RH. This was the closest to pure sinusoidal waveform among other waveforms.

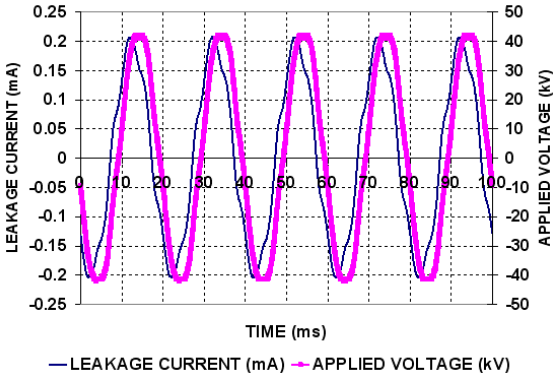

Fig. 8: *The applied voltage and leakage current waveforms of high RH first withdrawal polluted insulator*

Table 1: *The correlation coefficients of the new-clean insulator leakage current measurement results*

Variables	V_{max}	I_{max}	H	T	P	θ	Cos (θ)	H1	H3	H5	H7	H9	H11	H13	THD
V_{max}	1	0.73	-0.07	-0.06	0.12	0.22	-0.21	0.76	0.59	0.93	0.88	0.39	0.92	0.88	0.44
I_{max}	0.73	1	0.56	-0.29	0.14	-0.47	0.47	1.00	0.94	0.92	0.91	0.80	0.74	0.81	-0.26
H	-0.07	0.56	1	-0.37	0.10	-0.88	0.87	0.54	0.59	0.24	0.24	0.54	0.00	0.19	-0.83
T	-0.06	-0.29	-0.37	1	0.08	0.24	-0.25	-0.28	-0.33	-0.20	-0.22	-0.37	-0.08	-0.09	0.31
P	0.12	0.14	0.10	0.08	1	-0.06	0.05	0.15	0.08	0.13	0.16	0.00	0.10	0.15	-0.03
θ	0.22	-0.47	-0.88	0.24	-0.06	1	-1.00	-0.43	-0.55	-0.11	-0.12	-0.60	0.13	-0.05	0.88
Cos (θ)	-0.21	0.47	0.87	-0.25	0.05	-1.00	1	0.43	0.56	0.11	0.12	0.61	-0.13	0.05	-0.89
H1	0.76	1.00	0.54	-0.28	0.15	-0.43	0.43	1	0.92	0.94	0.92	0.78	0.76	0.83	-0.22
H3	0.59	0.94	0.59	-0.33	0.08	-0.55	0.56	0.92	1	0.82	0.81	0.93	0.53	0.62	-0.38
H5	0.93	0.92	0.24	-0.20	0.13	-0.11	0.11	0.94	0.82	1	0.98	0.65	0.89	0.89	0.12
H7	0.88	0.91	0.24	-0.22	0.16	-0.12	0.12	0.92	0.81	0.98	1	0.67	0.86	0.86	0.08
H9	0.39	0.80	0.54	-0.37	0.00	-0.60	0.61	0.78	0.93	0.65	0.67	1	0.36	0.43	-0.49
H11	0.93	0.74	0.00	-0.08	0.10	0.13	-0.13	0.76	0.53	0.89	0.86	0.36	1	0.94	0.38
H13	0.88	0.81	0.19	-0.09	0.15	-0.05	0.05	0.83	0.62	0.89	0.86	0.94	0.94	1	0.23
THD	0.44	-0.26	-0.83	0.31	-0.03	0.88	-0.89	-0.22	-0.38	0.12	0.08	0.38	0.38	0.23	1

The more pure sinusoidal waveform property is also indicated by frequency spectrum on Figure 9. It is shown that after the fundamental, the second highest was fifth harmonics. Nevertheless, this fifth harmonics was very small, only 7.3%, indicated that the leakage current waveform tent to be pure sinusoidal relatively.

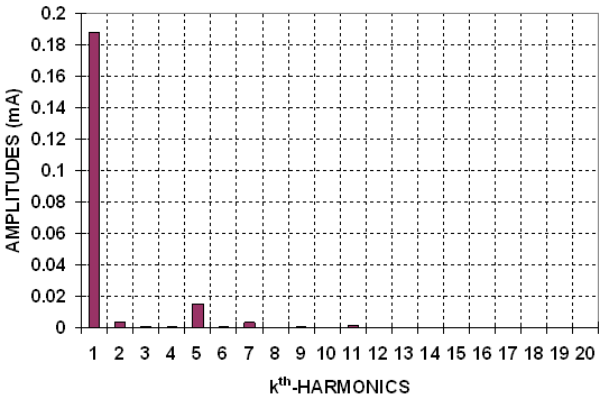

Fig.9: *The frequency spectrum of leakage current waveforms of high RH first withdrawal insulator*

Table 2 shows the correlation coefficients of the first withdrawal porcelain insulator based on 39 data of leakage current measurements with various temperature, humidity, pressure and applied voltage amplitude. H (relative humidity) had small values of correlation coefficients to other parameters, except to T (temperature). Of course, if the temperature increased, the relative humidity would reduce considerably. The relative humidity had small correlation coefficients to leakage current amplitude and phase angle or power factor. This did not mean that the relative humidity had very small influence both parameters, but there was another parameter, beside both parameters, which was pollutant, adhered on the insulator surface. On high relative humidity, the pollutant influenced the leakage current amplitudes and the phase angles were very significant. The former would increase and the latter would reduce extremely. The first withdrawal insulator was carried out on high dry season weather condition and to be further carried out measurement in the laboratory. Thus the leakage current waveform was the closest to pure sinusoidal on high humidity, among other withdrawals, including the new-clean porcelain insulator.

As other representations, the correlations among parameters are also shown by principal component analysis on Figure 10. In this figure, it is shown that THD close to PHA (phase angle). If the phase angle increased, which was accompanied by THD. Other conditions, similar as described on the correlation coefficient above. Pressure (P) close to the central coordinate, that it meant practically no influence other parameters. This PCA indicates that PHA (phase angle) closed to THD. This meant that THD was proportional to PHA very significantly. Usually THD would increase if the phase angle rose. A high phase angle represented a high capacitive of insulator. Thus, on the high capacitive condition of insulator, THD was also high. Humidity (H) opposites to temperature (T), so that the humidity would reduce as the temperature increased. The leakage current amplitude (Imax) closes to first (H1) and third (H3) harmonics. This meant the first and third harmonics would rise as leakage current amplitude increased. The leakage current amplitude is far from the applied voltage and humidity. This meant, although the leakage current was influenced by both quantities, there was other quantity, namely pollutant adhered on the insulator surface which had important role to increase the leakage current amplitude.

Table 3 lists the EDAX test results of pollutant adhered on first withdrawal porcelain insulator. It is seen that the highest chemical content was iron, which supposed it was from, surrounding metal,

Table 2: *Correlation coefficients of first withdrawal insulator*

Variables	V_{max}	I_{max}	H	T	P	θ	Cos (θ)	H1	H3	H5	H7	H9	H11	H13	THD
V_{max}	1	0.23	-0.41	0.22	-0.26	0.27	-0.34	0.22	0.20	0.28	0.31	0.23	0.24	0.18	0.13
I_{max}	0.23	1	-0.33	0.59	-0.09	-0.76	0.73	1.00	0.87	0.94	0.86	0.65	0.88	0.32	-0.78
H	-0.41	-0.33	1	-0.85	0.09	-0.13	0.12	-0.31	-0.13	-0.58	-0.70	-0.69	-0.65	-0.33	-0.03
T	0.22	0.59	-0.85	1	-0.08	-0.24	0.25	0.56	0.43	0.79	0.86	0.77	0.85	0.45	-0.28
P	-0.26	-0.09	0.09	-0.08	1	0.01	-0.01	-0.09	0.00	-0.12	-0.11	-0.01	-0.08	-0.30	-0.03
θ	0.27	-0.76	-0.13	-0.24	0.01	1	-1.00	-0.78	-0.67	-0.57	-0.43	-0.20	-0.51	-0.11	0.97
Cos (θ)	-0.34	0.73	0.12	0.25	-0.01	-1.00	1	0.74	0.62	0.55	0.41	0.19	0.50	0.12	-0.96
H1	0.22	1.00	-0.31	0.56	-0.09	-0.78	0.74	1	0.87	0.93	0.84	0.63	0.87	0.30	-0.80
H3	0.20	0.87	-0.13	0.43	0.00	-0.67	0.62	0.87	1	0.78	0.68	0.43	0.76	0.20	-0.63
H5	0.28	0.94	-0.58	0.79	-0.12	-0.57	0.55	0.93	0.78	1	0.98	0.82	0.97	0.46	-0.58
H7	0.31	0.86	-0.70	0.86	-0.11	-0.43	0.41	0.84	0.68	0.98	1	0.88	0.97	0.49	-0.44
H9	0.23	0.65	-0.69	0.77	-0.01	-0.20	0.19	0.63	0.43	0.82	0.88	1	0.82	0.37	-0.21
H11	0.24	0.88	-0.65	0.85	-0.08	-0.51	0.50	0.87	0.76	0.97	0.97	0.82	1	0.36	-0.52
H13	0.18	0.32	-0.33	0.45	-0.30	-0.11	0.12	0.30	0.20	0.46	0.49	0.37	0.36	1	-0.07
THD	0.13	-0.78	-0.03	-0.28	-0.03	0.97	-0.96	-0.80	-0.63	-0.58	-0.44	-0.21	-0.52	-0.07	1

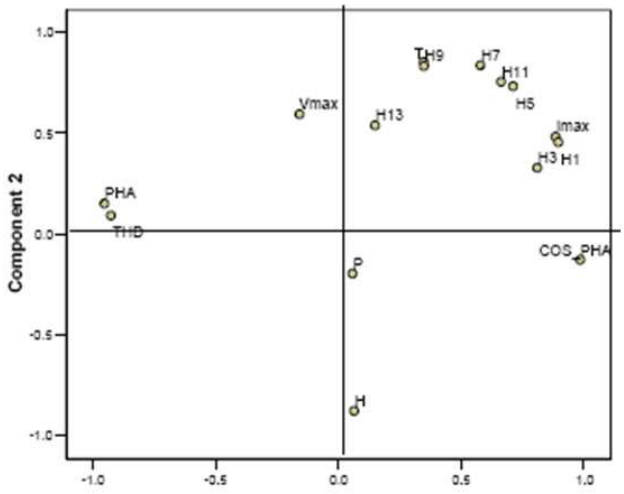

Fig.10: *PCA of first withdrawal porcelain insulator*

ground and even emission from geothermal power plant. Even so, other chemical elements, especially chlorine, were originally supposed from geothermal power plant.

Table 3: *Pollutant test results of first withdrawal porcelain insulator*

Elements	Test-1 (%)	Test-2 (%)	Average (%)
Al	6.64	7.88	7.26
Si	20.0	16.51	18.255
K	11.62	6.54	9.08
Ca	13.74	7.18	10.46
Fe	34.17	53.95	44.06
Zn	9.88	5.72	7.80
Cl	3.94	2.21	3.075

3.3 The Second Withdrawal Polluted Insulator

Whereas, Figure 11 is the leakage current waveform of second withdrawal of porcelain insulator, which carried out on December 4^{th}, 2007. As a sample of measurement of leakage current, it was on high humidity condition. This condition was 99% RH, 28.9oC, 34.4 kV_{max} and without pressure. The harmonics were 86.59%, 0.72%, 15.58%, 5.33%, 0.80%, 2.36% and 0.43% compared to the leakage current amplitude. Whereas, the leakage current amplitude was 27.6 A. Then, the THD and the phase angle were 19.3% and 66.8 degree respectively.

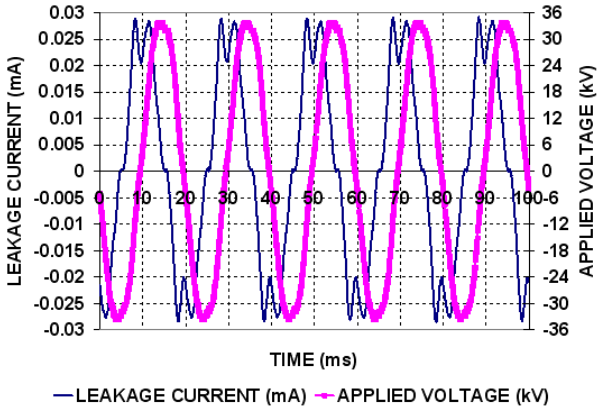

Fig.11: *The applied voltage and LC waveforms of high RH second withdrawal polluted insulator*

Figure 12 shows the frequency spectrum of the leakage current waveform as shown by Figure 11. It is shown that the fifth and seventh harmonics were also dominant, after the fundamental. This occurrence was caused by the leakage current waveform of Figure 11 rather far from pure sinusoidal waveform. In this condition, the insulator was still in capacitive property, due to less pollutant on the insulator sur-

Table 4: *The correlation coefficients of second withdrawal insulator*

Variables	V_{max}	T	H	P	I_{max}	θ	Cos (θ)	H1	H3	H5	H7	H9	H11	H13	THD
V_{max}	1	-0.17	-0.40	-0.11	0.20	0.48	-0.47	0.08	0.18	0.71	0.77	0.38	0.62	0.48	0.64
T	-0.17	1	-0.12	0.01	-0.25	0.21	-0.22	-0.25	-0.09	-0.29	-0.36	0.05	-0.23	-0.36	0.08
H	-0.40	-0.12	1	0.16	0.51	-0.74	0.72	0.55	0.28	0.07	-0.16	0.04	0.09	-0.03	-0.73
P	-0.11	0.01	0.16	1	0.13	-0.16	0.15	0.14	0.01	0.00	-0.06	-0.20	0.05	0.04	-0.19
I_{max}	0.20	-0.25	0.51	0.13	1	-0.65	0.65	0.98	0.73	0.71	0.57	0.43	0.71	0.43	-0.56
θ	0.48	0.21	-0.74	-0.16	-0.65	1	-1.00	-0.72	-0.29	-0.11	0.04	0.06	-0.19	-0.12	0.94
Cos (θ)	-0.47	-0.22	0.72	0.15	0.65	-1.00	1	0.71	0.28	0.11	-0.03	-0.06	0.20	0.13	-0.93
H1	0.08	-0.25	0.55	0.14	0.98	-0.72	0.71	1	0.72	0.69	0.55	0.40	0.70	0.44	-0.63
H3	0.18	-0.09	0.28	0.01	0.73	-0.29	0.28	0.72	1	0.55	0.52	0.69	0.50	0.11	-0.24
H5	0.71	-0.29	0.07	0.00	0.71	-0.11	0.11	0.69	0.55	1	0.91	0.49	0.90	0.61	0.09
H7	0.77	-0.36	-0.16	-0.06	0.57	0.04	-0.03	0.55	0.52	0.91	1	0.49	0.89	0.73	0.23
H9	0.38	0.05	0.04	-0.20	0.43	0.06	-0.06	0.40	0.69	0.49	0.49	1	0.47	0.08	0.12
H11	0.62	-0.23	0.09	0.05	0.71	-0.19	0.20	0.70	0.50	0.90	0.89	0.47	1	0.75	0.01
H13	0.48	-0.36	-0.03	0.04	0.43	-0.12	0.13	0.44	0.11	0.73	0.73	0.08	0.75	1	0.01
THD	0.64	-0.08	-0.73	-0.56	-0.56	0.94	-0.93	-0.63	-0.24	0.09	0.23	-0.12	-0.01	-0.01	1

face. This was caused by the withdrawal of insulator was carried out in rainy season. Thus, the insulator was still relatively clean, so that the effect of high humidity was relatively low.

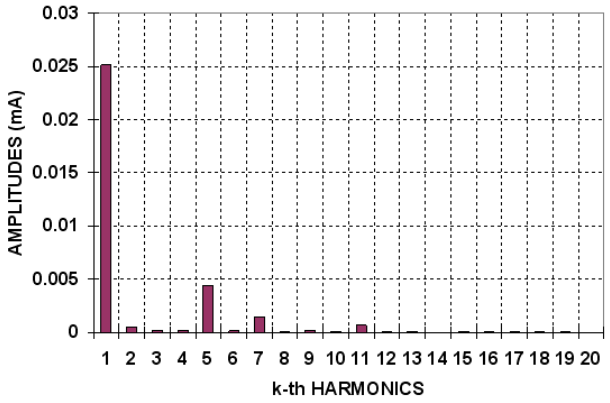

Fig.12: *The frequency spectrum of leakage current waveforms of high RH second withdrawal insulator*

Table 4 is the correlation coefficient matrix of the parameters for second withdrawal insulator, obtained from 121 data of leakage current measurements. In this condition, the relative humidity (H) significantly correlated to the leakage current amplitude and the phase angle or the power factor. The correlation coefficient values were 0.51 and -0.74 or 0.72 respectively. If the humidity increased, the leakage current amplitude would rise and the phase angle would reduce or power factor would increase considerably. Otherwise, the THD was also influenced by the humidity significantly, indicated by the value of -0.73. If the humidity increased, the leakage current wave would tend to be pure sinusoidal form relatively.

These correlations among parameters are also shown by principal component analysis (PCA) on Figure 13, for second withdrawal insulator. In this figure, it is shown that the THD close to PHA (phase angle). The phase angle increased, accompanied by THD. No doubt, the power factor (PF) opposites with the phase angle (PH). The phase angle relatively close to H (humidity), that if the humidity increased, the power factor would increase too slightly. The pressure (P) closes to the central point of coordinate, it meant the pressure did not practically influence other parameters.

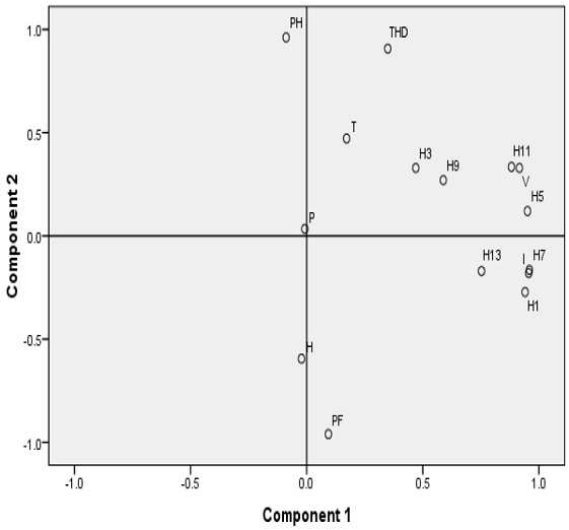

Fig.13: *The PCA of second withdrawal insulator*

Table 5 indicates the EDAX test results of pollutant adhered on the second withdrawal porcelain insulator surface. It is seen that the highest chemical content was also iron, similar with the first withdrawal, which also supposed it was from surrounding metal, ground and even emission from geothermal power plant.

3.4 The Third Withdrawal Polluted Insulator

Figure 14 presents the waveforms of porcelain insulator for third withdrawal on 18^{th} March 2008. This

Table 5: *Pollutant test results of second withdrawal insulator*

Elements	Test-1 (%)	Test-2 (%)	Average (%)
Al	5.06	5.06	5.06
Si	11.1	11.1	11.1
Ca	6.66	6.66	6.66
Fe	70.45	70.45	70.45
Na	3.14	3.14	3.14

condition was on 99%, 25.8oC, 15.6kPa, and 34.44 kV_{max}. The leakage current harmonics were 90.52%, 0.60%, 8.59%, 2.38%, 0.43%, 0.91% and 0.04% compared to the leakage current amplitude. Whereas, the leakage current amplitude was 67.2 A. Otherwise, the THD and the phase angle were 9.93% and 25.69 degree respectively.

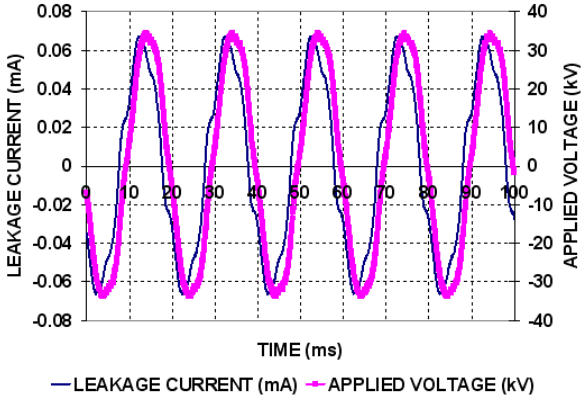

Fig.14: *The applied voltage and leakage current waveforms of high RH third withdrawal insulator*

Figure 15 shows frequency spectrum of leakage current waveform as shown by Figure 14. It is shown that the fifth and seventh harmonics were also dominant, after the fundamental. However, their percentages to the fundamental were lower than the second withdrawal. This meant the leakage current waveform was more pure sinusoidal rather than the second withdrawal, although both were on high humidity.

Table 6 is correlation coefficient matrix of parameters for third withdrawal insulator. In this condition, the relative humidity (H) did not reveal clearly to influence to leakage current amplitude and/or phase angle. Nevertheless, actually it influenced both parameters. This occurred was caused the pollutant adhered on the insulator surface dominantly.

These correlations are also shown by principal component analysis (PCA) on Figure 16 for third withdrawal insulator. In this figure, it is shown that the THD also close to PH (phase angle). The phase angle increased, accompanied by THD. Thus, the power factor (PF) opposites to the phase angle (PH). The temperature (T) opposites to humidity (H), as

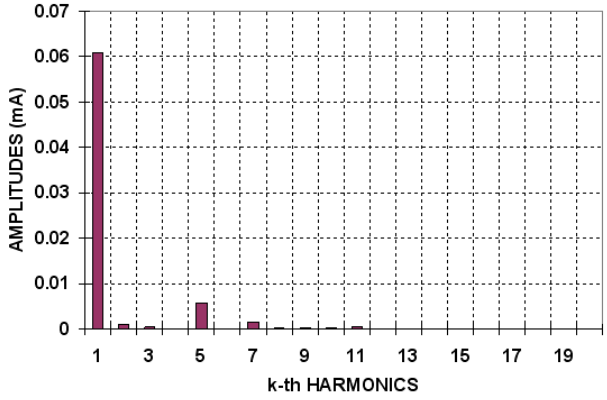

Fig.15: *The frequency spectrum of leakage current waveforms of high RH third withdrawal insulator*

representation of both behaviors. If the temperature increased, the humidity would reduce. The leakage current amplitude (I) closes to the first harmonic amplitude (H1). Thus, the first harmonic amplitude was highly specified by the leakage current amplitude. The first harmonic amplitude would rise as the leakage current amplitude increased, and vice versa. Otherwise, the pressure closes to the central coordinate, which meant it did not practically influence other parameter(s).

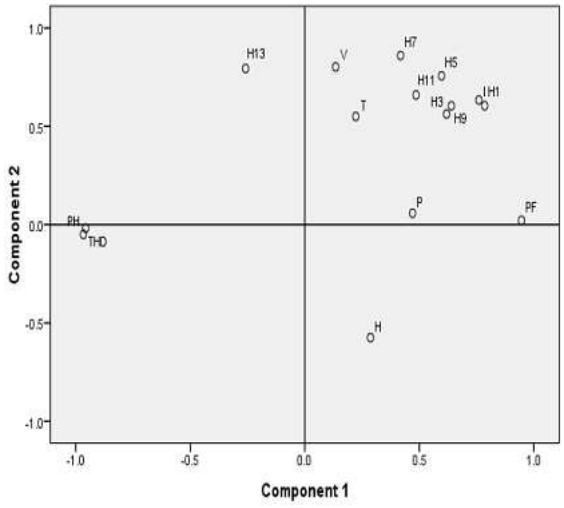

Fig.16: *The PCA of third withdrawal insulator*

Table 7 indicates the EDAX test results of pollutant adhered on third withdrawal porcelain insulator. It is seen that iron was available, although it was not the highest chemical element. Aluminum was also available. These were supposed it was from surrounding metal, ground and even emission from geothermal power plant.

Table 6: *The correlation coefficients of third withdrawal insulator*

Variables	V_{max}	T	H	P	I_{max}	θ	Cos (θ)	H1	H3	H5	H7	H9	H11	H13	THD
V_{max}	1	0.08	-0.03	0.01	0.60	-0.17	0.14	0.58	0.50	0.82	0.87	0.64	0.55	0.61	-0.01
T	0.08	1	-0.78	0.18	0.52	-0.27	0.27	0.51	0.33	0.39	0.45	0.33	0.59	0.30	-0.42
H	-0.03	-0.78	1	0.01	-0.16	-0.24	0.25	-0.14	-0.11	-0.09	-0.23	-0.10	-0.36	-0.41	-0.09
P	0.01	0.18	0.01	1	0.41	-0.31	0.28	0.42	0.41	0.27	0.19	0.28	0.31	-0.08	-0.41
I_{max}	0.60	0.52	-0.16	0.41	1	-0.75	0.71	0.99	0.87	0.93	0.85	0.86	0.76	0.30	-0.74
θ	-0.17	-0.27	-0.24	-0.31	-0.75	1	-1.00	-0.77	-0.58	-0.63	-0.46	-0.60	-0.47	0.14	0.96
Cos (θ)	0.14	0.27	0.25	0.28	0.71	-1.00	1	0.73	0.53	0.59	0.43	0.56	0.44	-0.14	-0.95
H1	0.58	0.51	-0.14	0.42	0.99	-0.77	0.73	1	0.86	0.93	0.83	0.87	0.77	0.26	-0.76
H3	0.50	0.33	-0.11	0.41	0.87	-0.58	0.53	0.86	1	0.80	0.68	0.73	0.53	0.36	-0.57
H5	0.82	0.39	-0.09	0.27	0.93	-0.63	0.59	0.93	0.80	1	0.96	0.84	0.71	0.49	-0.54
H7	0.87	0.45	-0.23	0.19	0.85	0.46	0.43	0.83	0.68	0.96	1	0.80	0.74	0.57	-0.38
H9	0.64	0.33	-0.10	0.28	0.86	0.60	0.56	0.87	0.73	0.84	0.80	1	0.75	0.20	-0.56
H11	0.55	0.59	-0.36	0.31	0.76	-0.47	0.44	0.77	0.53	0.71	0.74	0.75	1	0.21	-0.48
H13	0.61	0.30	-0.41	-0.08	0.30	0.14	-0.14	0.26	0.36	0.49	0.57	0.20	0.21	1	0.21
THD	-0.01	-0.42	-0.09	-0.41	-0.74	0.96	-0.95	-0.76	-0.57	-0.54	-0.38	-0.56	-0.48	0.21	1

Table 7: *Pollutant testing results of third withdrawal insulator*

Elements	Test-1 (%)	Test-2 (%)	Average (%)
Al	14.77	12.26	13.52
Si	70.38	59.60	64.99
Ca	8.48	7.21	7.85
Fe	0	15.14	7.57
K	6.37	5.79	6.08

3.5 The Polluted Fourth Withdrawal Insulator

The next withdrawal was fourth, on 22^{nd} August 2008. Figure 17 presents the waveforms of fourth withdrawal porcelain insulator. This condition was on 99%, 23.7°C, 31.92 kV_{max} and without pressure. The harmonics were 87.3 μA, 0.43 μA, 9.89 μA, 2.52 μA, 0.324 μA, 1.350 μA and 0.182 μA. The leakage current amplitude was 140 μA, and the THD and the phase angle were 11.8% and 29.46 degree respectively.

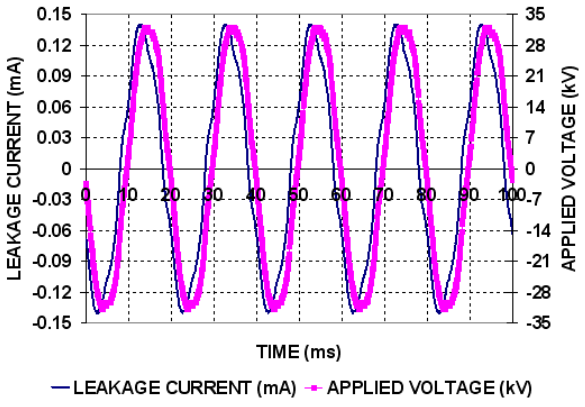

Fig.17: *The applied voltage and leakage current waveforms of high RH fourth withdrawal insulator*

Figure 18 shows the frequency spectrum of leakage current waveform as shown by Figure 16. It is shown that the fifth and seventh harmonics were also dominant, after the fundamental. Nevertheless, their percentages to the fundamental were lower than the second withdrawal insulator. In other word, the leakage current waveform was more pure sinusoidal rather than the second withdrawal, both were on high humidity.

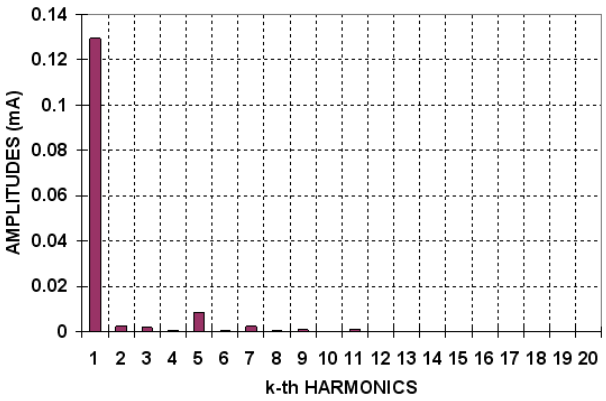

Fig.18: *Frequency spectrum of leakage current waveforms of high RH fourth withdrawal insulator*

Table 8 is the correlation coefficient matrix of parameters for fourth withdrawal insulator. In this case, the relative humidity (H) did not reveal clearly to influence to leakage current amplitude. This was caused by adhered pollutant on the insulator surface. Nevertheless, it clearly influenced to the phase angle or the power factor, which indicated by -0.70 and 0.69 of correlation coefficient values respectively. If the humidity rose, the phase angle would reduce or the power factor would increase significantly. Besides that, the humidity highly influenced the THD, which was indicated by -0.64 of correlation coefficient. The THD would reduce significantly, as humidity increased.

Besides indicated by the correlation coefficients on

Table 8: *The correlation coefficients of fourth withdrawal insulator*

Variables	V_{max}	T	H	P	I_{max}	θ	Cos (θ)	H1	H3	H5	H7	H9	H11	H13	THD
V_{max}	1	0.118	0.00	-0.06	0.23	-0.08	0.08	0.21	-0.24	0.44	0.48	0.20	0.38	0.31	-0.22
T	0.11	1	-0.48	-0.15	0.40	-0.15	0.18	0.41	-0.12	0.61	0.42	0.33	0.66	0.46	-0.23
H	0.00	-0.48	1	0.18	0.20	-0.70	0.69	0.20	-0.28	-0.15	-0.33	-0.28	-0.23	-0.38	-0.64
P	-0.06	-0.15	0.18	1	0.16	-0.21	0.19	0.09	-0.40	-0.10	-0.29	-0.33	-0.15	-0.45	-0.12
I_{max}	0.23	0.40	0.20	0.16	1	-0.74	0.74	0.97	-0.03	0.84	0.56	0.46	0.78	0.28	-0.67
θ	-0.08	-0.15	-0.70	-0.21	-0.74	1	-1.00	-0.74	0.26	-0.41	-0.08	-0.05	-0.35	0.08	0.93
Cos (θ)	0.08	0.18	0.69	0.19	0.74	-1.00	1	0.74	-0.27	0.43	0.10	0.07	0.38	-0.05	-0.94
H1	0.21	0.41	0.20	0.09	0.97	-0.74	0.74	1	0.03	0.83	0.57	0.52	0.77	0.23	-0.69
H3	-0.24	-0.12	-0.28	-0.40	-0.03	0.26	-0.27	0.03	1	0.02	0.32	0.60	0.05	0.31	0.27
H5	0.44	0.61	-0.15	-0.10	0.84	-0.41	0.43	0.83	0.02	1	0.86	0.68	0.96	0.60	-0.41
H7	0.48	0.42	-0.33	-0.29	0.56	-0.08	0.10	0.57	0.32	0.86	1	0.87	0.84	0.74	-0.09
H9	0.20	0.33	-0.28	-0.33	0.46	-0.05	0.07	0.52	0.60	0.68	0.87	1	0.68	0.61	-0.06
H11	0.38	0.66	-0.23	-0.15	0.78	-0.35	0.38	0.77	0.05	0.96	0.84	0.68	1	0.62	-0.38
H13	0.31	0.46	-0.38	-0.45	0.28	0.08	-0.05	0.23	0.31	0.60	0.74	0.61	0.62	1	0.06
THD	-0.22	-0.23	-0.64	-0.12	-0.67	0.93	-0.94	-0.69	0.27	-0.41	-0.09	-0.06	-0.38	0.06	1

Table 8, the dependence among parameters are also shown by principal component analysis (PCA) on Figure 19 for fourth withdrawal insulator. In this figure, it is shown that the THD also close to PH (phase angle). The phase angle increased, accompanied by THD. Thus, the power factor (PF) opposites to the phase angle (PH). Nevertheless, both THD and PH opposite to the leakage current amplitude (I). The leakage current amplitude increased, the THD and the phase angle would reduce considerably. The first harmonic is very close to the leakage current amplitude (I), so that the first harmonic was specified by the leakage current amplitude (I) very dominantly.

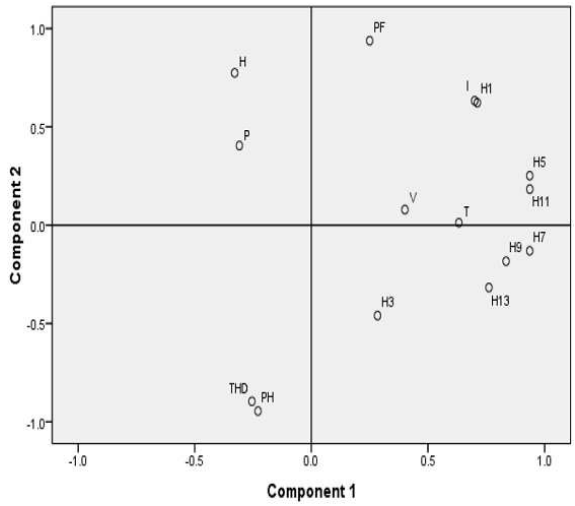

Fig.19: *The PCA of fourth withdrawal insulator*

Table 9 indicates the EDAX test results of adhered pollutant on fourth withdrawal porcelain insulator. It is seen that iron was available as the second highest chemical element, after silicon. Aluminum was also available as medium content. These were supposed they were from surrounding metal, ground and even emission from geothermal power plant.

Table 9: *Pollutant testing results of fourth withdrawal insulator*

Elements	Test-1 (%)	Test-2 (%)	Average (%)
Al	15.30	19.28	17.29
Si	34.25	43.61	38.93
K	3.14	3.03	3.085
Ca	4.83	5.90	5.365
Fe	42.48	28.18	35.33

3.6 The Fifth Withdrawal Polluted Insulator

The fifth withdrawal insulator was carried out on December 18^{th}, 2008. As an example of measurement results on high humidity, it is shown the leakage current waveform by Figure 20, on 99%, 30.5°C, 36.12 kV_{max} for relative humidity, temperature and applied voltage amplitude respectively, and without pressure. The phase angle was 29.56 degree. Whereas Figure 21 is the spectrum frequency of the leakage current wave. The first to thirteenth odd harmonics amplitudes were 87.2%, 2.9%, 5.8%, 1.7%, 0.6%, 0.6%, 1.1% and 0.4% respectively compared to the leakage current amplitude, and the leakage current amplitude itself was 44.8 μA. Thus, the THD was 7.8%.

It is shown that the fifth and followed by third harmonics were also dominant, after the fundamental. The third harmonics has been visible slightly.

Table 10 indicates the correlation coefficient values among parameters. It is seen that the humidity most significantly influence the power factor of insulator leakage current, among other parameters. If the humidity increased, the power factor would increase too. The phase angle was very tight with the THD. If the phase angle increased, the THD would increase too, and vice versa.

Figure 22 shows the PCA, which support the correlation coefficient values as indicated on Table 10. It

Table 10: *The correlation coefficients of fifth withdrawal insulator*

Variables	V_{max}	T	H	P	I_{max}	PHA	COS PHI	H1	H3	H5	H7	H9	H11	H13	THD
V	1	0.08	-0.02	0.06	0.21	-0.16	0.18	0.21	-0.10	0.72	0.53	0.20	0.54	0.28	-0.27
T	0.08	1	-0.49	0.66	0.93	-0.53	0.43	0.93	0.79	0.67	0.69	0.20	0.61	0.80	-0.50
H	-0.02	-0.49	1	-0.44	-0.31	-0.38	0.49	-0.32	-0.22	-0.44	-0.66	0.42	-0.38	-0.30	-0.35
P	0.06	0.66	-0.44	1	0.65	-0.34	0.24	0.66	0.52	0.50	0.54	0.04	0.24	0.62	-0.33
I	0.21	0.93	-0.31	0.65	1	-0.69	0.60	1.00	0.83	0.76	0.70	0.36	0.54	0.92	-0.65
PHA	-0.16	-0.53	-0.38	-0.34	-0.69	1	-0.99	-0.69	-0.57	-0.37	-0.14	-0.59	-0.17	-0.61	0.92
COS PHI	0.18	0.43	0.49	0.24	0.60	-0.99	1	0.60	0.48	0.30	0.04	0.59	0.15	0.52	-0.92
H1	0.21	0.93	-0.32	0.66	1.00	-0.69	0.60	1	0.82	0.76	0.70	0.35	0.53	0.92	-0.66
H3	-0.10	0.79	-0.22	0.52	0.83	-0.57	0.48	0.82	1	0.44	0.49	0.44	0.36	0.80	-0.36
H5	0.72	0.67	-0.44	0.50	0.76	-0.37	0.30	0.76	0.44	1	0.89	0.19	0.74	0.75	-0.41
H7	0.53	0.69	-0.66	0.54	0.70	-0.14	0.04	0.70	0.49	0.89	1	0.05	0.66	0.73	-0.15
H9	0.20	0.20	0.42	0.04	0.36	-0.59	0.59	0.35	0.44	0.19	0.05	1	0.06	0.45	-0.48
H11	0.54	0.61	-0.38	0.24	0.54	-0.17	0.15	0.53	0.36	0.74	0.66	0.06	1	0.37	-0.17
H13	0.28	0.80	-0.30	0.62	0.92	-0.61	0.52	0.92	0.80	0.75	0.73	0.45	0.37	1	-0.56
THD	-0.27	-0.50	-0.35	-0.33	-0.65	0.92	-0.92	-0.66	-0.36	-0.41	-0.15	-0.48	-0.17	-0.56	1

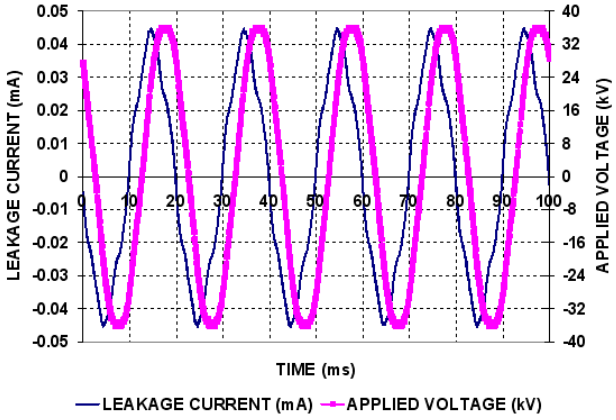

Fig.20: *The applied voltage and leakage current waveforms of high RH fifth withdrawal insulator*

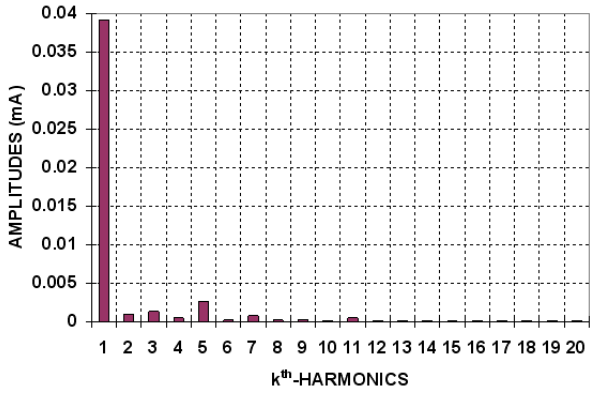

Fig.21: *Frequency spectrum of leakage current waveforms of high RH fifth withdrawal insulator*

is shown that the THD was very close to PHA (phase angle). The relative humidity (H) was rather close to the power factor (PF), rather than other parameters.

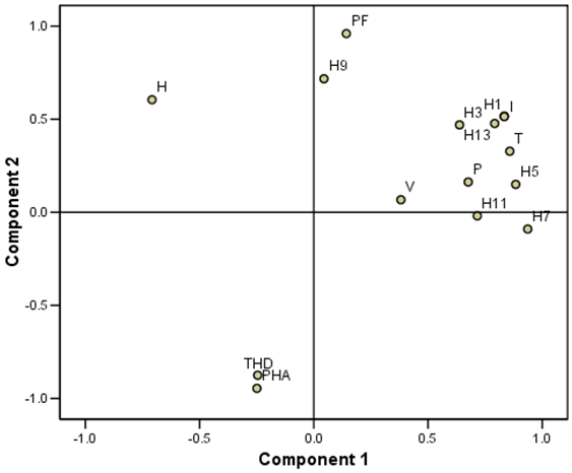

Fig.22: *The PCA of fifth withdrawal insulator*

Table 11 indicates the EDAX test results of adhered pollutant on the fifth withdrawal porcelain insulator. It is seen that iron was as the second highest chemical element, after silicon. Aluminum was also available as medium content. Besides that, sulfur element was also existed, in medium composition, which supposed explicitly from emission of geothermal power plant.

3.7 The Sixth Withdrawal Polluted Insulator

The sixth withdrawal porcelain insulator was taken from site on April 7^{th}, 2009. The influence of pollutant to the leakage current of insulator was less than that the first withdrawal insulator. When insulator withdrawal, the weather was dominated by a rainy season. As an example of measurement on high humidity, it was on 99%, 27.1°C, 32.25 kV_{max} for relative humidity, temperature and applied voltage

Table 11: *Pollutant testing results of fifth withdrawal insulator*

Elements	Test-1 (%)	Test-2 (%)	Average (%)
Mg	2.25	2.53	2.39
Al	17.97	17.90	17.935
Si	41.71	41.59	41.65
S	9.44	9.78	9.61
Cl	0.76	0.65	0.705
K	2.9	2.68	2.79
Ca	2.54	2.44	2.49
Ti	1.65	2.10	1.875
Fe	20.78	20.32	20.55

amplitude respectively, and without pressure, where the applied voltage and leakage current waveforms are shown on Figure 23, with the phase angle was 50.9 degree.

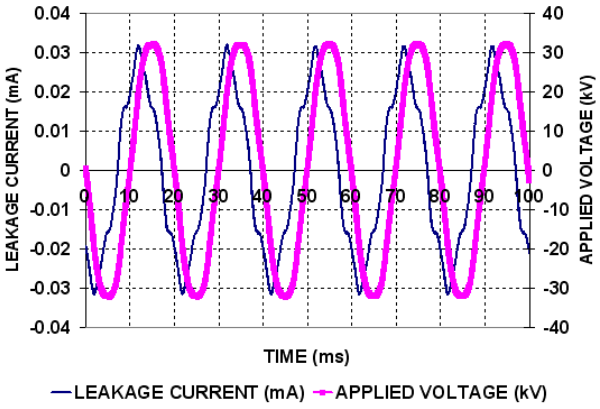

Fig.23: *The leakage current waveform of high humidity sixth withdrawal insulator*

Figure 24 shows the frequency spectrum of leakage current waveform of Figure 23. It is shown that the fifth harmonics was also dominant, after the fundamental. However, other harmonics were very low. Therefore, in this withdrawal insulator, the influence of pollutant was lower than that on the fifth withdrawal insulator. The first to thirteenth odd harmonics amplitudes were 82.8%, 1.2%, 9.9%, 1.7%, 0.2%, 1.6% and 0.1% to the leakage current amplitude respectively. Whereas, the leakage current amplitude, insulator impedance and the THD were 32 μA, 1,007,812,500 Ω and 12.4% respectively.

Table 12 shows the parameter correlation coefficient values of sixth withdrawal insulator. It is seen that the highest significant influence of humidity was the power factor (COS PHI) of insulator leakage current. The phase angle (PHA) was very tight correlation with the THD. If the phase angle reduced, the THD would decrease too.

Figure 25 shows the PCA scatter plot parameters of sixth withdrawal porcelain insulator. THD is very

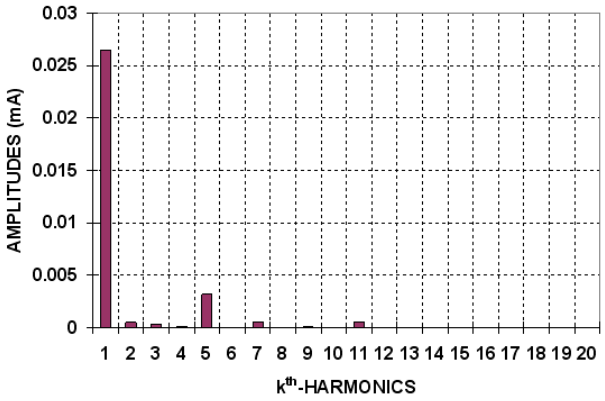

Fig.24: *Frequency spectrum of leakage current waveforms of high humidity sixth withdrawal insulator*

close to the phase angle (PHA). Otherwise, the humidity (H) is rather close to the power factor (PF). Therefore, both important phenomena support the correlation coefficient values on Table 12.

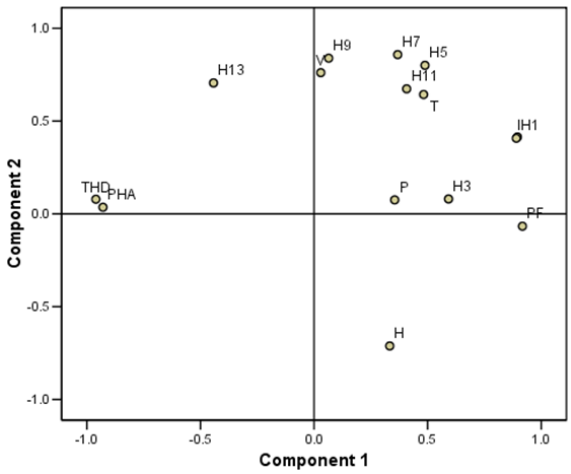

Fig.25: *The PCA of sixth withdrawal insulator*

Table 13 indicates the EDAX test results of adhered pollutant on the fifth withdrawal porcelain insulator. It is seen that silicon and iron were as the high chemical element composition. Aluminium was also available as medium content. Besides that, sulfur element was also existed as medium composition too, which supposed explicitly from emission of geothermal power plant. The chemical elements of silicon (Si), iron (Fe) and aluminium (Al) were supposed from the grounding, metal surrounding the insulators and/or from geothermal emission.

According to the correlation coefficient matrices and principal component analyses, the relative humidity close to the power factor, the phase angle close to the THD, the pressure close to the center point and the harmonics close to the leakage current amplitude. These meant the power factor increased as the rela-

Table 12: *The correlation coefficients of sixth withdrawal insulator*

Variables	V_{max}	T	H	P	I_{max}	PHA	COS PHI	H1	H3	H5	H7	H9	H11	H13	THD
V	1	0.28	-0.27	0.03	0.32	-0.10	0.10	0.29	-0.16	0.74	0.67	0.50	0.64	0.56	0.08
T	0.28	1	-0.48	0.12	0.71	-0.35	0.33	0.72	0.51	0.72	0.64	0.65	0.44	0.16	-0.44
H	-0.27	-0.48	1	0.07	-0.04	-0.40	0.44	-0.04	-0.02	-0.29	-0.50	-0.65	-0.15	-0.52	-0.29
P	0.03	0.12	0.07	1	0.37	-0.19	0.16	0.38	0.27	0.17	0.26	0.21	0.01	-0.09	-0.36
I	0.32	0.71	-0.04	0.37	1	-0.79	0.76	1.00	0.57	0.77	0.67	0.40	0.62	-0.10	-0.85
PHA	-0.10	-0.35	-0.40	-0.19	-0.79	1	-0.98	-0.77	-0.35	-0.43	-0.36	0.06	-0.46	0.36	0.88
COS PHI	0.10	0.33	0.44	0.16	0.76	-0.98	1	0.74	0.31	0.40	0.32	-0.08	0.44	-0.37	-0.88
H1	0.29	0.72	-0.04	0.38	1.00	-0.77	0.74	1	0.60	0.75	0.65	0.41	0.58	-0.11	-0.85
H3	-0.16	0.51	-0.02	0.27	0.57	-0.35	0.31	0.60	1	0.31	0.23	0.30	0.08	-0.31	-0.55
H5	0.74	0.72	-0.29	0.17	0.77	-0.43	0.40	0.75	0.31	1	0.81	0.61	0.84	0.33	-0.35
H7	0.67	0.64	-0.50	0.26	0.67	-0.36	0.32	0.65	0.23	0.81	1	0.75	0.72	0.45	-0.29
H9	0.50	0.65	-0.65	0.21	0.40	0.06	-0.08	0.41	0.30	0.61	0.75	1	0.44	0.43	-0.02
H11	0.64	0.44	-0.15	0.01	0.62	-0.46	0.44	0.58	0.08	0.84	0.72	0.44	1	0.35	-0.26
H13	0.56	0.16	-0.52	-0.09	-0.10	0.36	-0.37	-0.11	-0.31	0.33	0.45	0.43	0.35	1	0.45
THD	0.08	-0.44	-0.29	-0.36	-0.85	0.88	-0.88	-0.85	-0.55	-0.35	-0.29	-0.02	-0.26	0.45	1

Table 13: *Pollutant testing results of sixth withdrawal insulator*

Elements	Test-1 (%)	Test-2 (%)	Average (%)
Al	8.89	10.83	9.86
Si	18.76	22.08	20.42
S	7.44	8.40	7.92
K	1.4	1.44	1.42
Ca	1.85	0	0.925
Fe	12.14	8	10.07

tive humidity rose, and the THD would rise if the phase angle increased. The pressure practically did not influence other parameter(s) significantly. The leakage current amplitudes influenced the harmonics generally. The leakage currents, which beside influenced by humidity, were also influenced by pollutant that indicated by the dry seasons. When withdrawal of insulators, it was in a dry season. The insulator was measured in high humidity, the leakage currents tent to be relatively pure sinusoidal. On this condition, the insulator property tent to be more conductive, rather than dry condition. Thus, if an insulator had high pollutant and high humidity simultaneously, the properties of leakage current would tend to be relatively pure sinusoidal or low THD, high amplitude, and low phase angle or high power factor. The temperature had an opposition characteristic with the humidity, namely if the temperature increased, the humidity would reduce, and consequently, the property of leakage current would be as above statements. The largest composition of chemical element was iron, after silicon. Sulfur was also existed, that supposed explicitly from emission of geothermal power plant.

3.8 The Seventh Withdrawal Polluted Insulator

The seventh withdrawal porcelain insulator was taken from site on August 12^{th}, 2009. The influence of pollutant to leakage current of insulator was similar with the first withdrawal insulator. The insulator was withdrawn on slightly dry season of weather. As an example of measurement on a high humidity, namely on 99%, 27.8°C, 28.9 kV_{max} for relative humidity, temperature and applied voltage amplitude respectively, and without pressure, the applied voltage and leakage current waveforms are shown on Figure 26, with the phase angle was 43.1 degree.

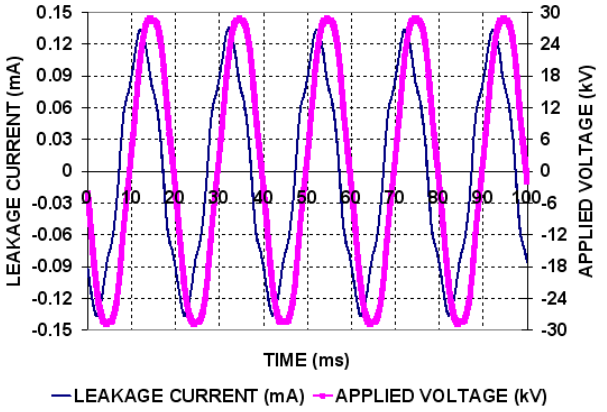

Fig.26: *The leakage current waveforms of high humidity seventh withdrawal insulator*

Figure 27 shows the frequency spectrum of leakage current waveform of Figure 26. It is shown that the fifth harmonic was also dominant, after the fundamental. Therefore, in this withdrawal insulator, the influence of pollutant was lower than that in the fifth withdrawal insulator. The first to thirteenth odd harmonics amplitudes were 90.15%, 0.39%, 7.26%, 1.15%, 0.33%, 0.71%, and 0.04% to the leakage current amplitude respectively. Whereas, the leakage current amplitude, the insulator impedance and the THD were 134 μA, 215 641 791 and 8.35% respectively.

Table 14 indicates the EDAX test results of ad-

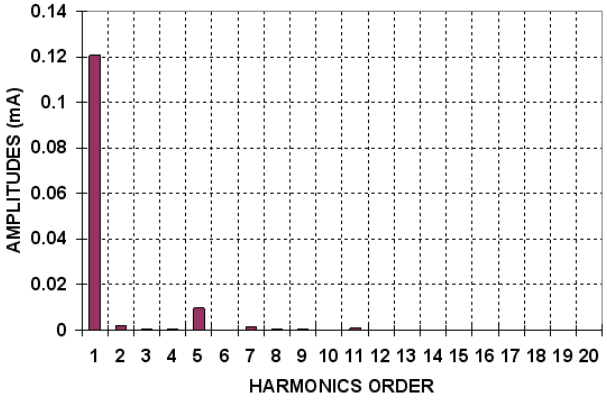

Fig.27: *The frequency spectrum of leakage current waveforms of high humidity seventh withdrawal insulator*

hered pollutant on the seventh withdrawal porcelain insulator. From these test results, it is shown that sulphur was the most dominant among chemical composition. This was very representative to the geothermal condition, due to typical chemical emission of geothermal area is sulphur. Silicon and ferrum were also dominant on second grade condition.

Table 14: *Pollutant testing results of seventh withdrawal insulator*

Elements	Test-1 (%)	Test-2 (%)	Average (%)
Al	9.01	8.30	8.655
Si	29.22	25.87	27.545
S	41.16	34.80	37.980
Fe	20.61	31.03	25.820

The leakage currents, which were beside influenced by humidity, were also influenced by pollutant that indicated by the dry season. Thus, on this insulator, the leakage current changed very significantly on high humidity, namely the insulator impedance was very low, only 215,641,791 Ω, and THD was also very low.

On this high humidity condition, the insulator property tent to be more conductive, rather than dry condition. Thus, if an insulator had high pollutant and high humidity simultaneously, the properties of leakage current were tendency to be relatively pure sinusoidal or low THD, high amplitude, and low phase angle or high power factor. Sulphur was existed, that supposed explicitly from emission of geothermal power plant. Generally, the influence of pollutant on the insulators was lower than that the insulators from coastal area.

Table 15 indicates the recapitulation of insulator impedances, phase angle and THD on the low and high humidity. Based on eight insulators, one new clean and seven polluted insulators, the most significant phenomena were occurred on seventh and first withdrawal insulators. These cases were indicated by the reduction of insulator impedances and THD, from low to high humidity, with impedance ratio of 0.1343 and 0.1363, and the THD ratio of 0.4598 and 0.3739 respectively. Both insulators were withdrawn on dry seasons. Furthermore, the second most significant phenomena were occurred on third and fourth withdrawal insulators. These cases were indicated by reduction of insulator impedance and phase angle on high humidity. These insulators were withdrawn on slightly dry season.

As the recapitulation of main chemical elements based on the average of eight insulator pollutants, it is listed by Table 16 below. Iron, silicon and aluminium were supposed mostly from the soil dust surrounding insulators. These chemical elements were in a small part from the geothermal area. Whereas, as a medium category of chemical elements, there were sulphur, calcium, kalium, natrium and chlorine. These chemical elements were supposed from the geothermal area, besides from the soil dust. Finally, as a small category, the chemical elements were zinc, magnesium and titan. These chemical elements were also supposed from the geothermal area, besides from the soil dust.

Table 16: *The recapitulation of main chemical elements of pollutant on the insulators*

The chemical elements of pollutant	Average percentage (%)
Fe	33.57
Si	27.44
Al	11.34
S	6.94
Ca	4.92
K	3.64
Na	2.33
Cl	1.70
Zn	0.98
Mg	0.30
Ti	0.23

As additional information of chemical content, it is listed the EDAX test results of scraped pollutant from installed insulators of switchyard equipment, such as arresters, CTs and CBs, as Table 17. The real pollutant stuck to equipment insulator surface, which was installed in the switchyard of Kamojang geothermal power plant is shown by Figure 28. Usually, the pollutant was on the top surface and on the tips of insulator sheds.

Table 17 lists the major chemical elements on the real pollutant that stuck on the switchyard equipment insulators. It is seen that silicon was also dominant, whereas sulphur was a medium chemical element composition on the pollutant. Thus, it strengthened above chemical element of insulator pollutant, which were installed by researchers.

In real condition on the sites, insulators are installed in some tens or decades of years, even in more

Table 15: *The recapitulation of insulator impedance, phase angle and THD on low and high humidity*

PORCELAIN INSULATOR	Z_{max} (Ω)	Z_{min} (Ω)	Z_{min}/Z_{max}	θ_{max} (deg) / pf_{min}	θ_{min} (deg) / pf_{max}	$(pf_{min})/(pf_{max})$	THD_{max} (%)	THD_{min} (%)	THD_{min} / THD_{max}
New-Clean	1 557 303 371	612 000 000	0.3930	86.6 / 0.06	46.7 / 0.69	0.0861	20.4	11.1	0.5427
1st withdrawal	1 496 250 000	203 883 495	0.1363	76.2 / 0.24	35.6 / 0.81	0.2934	22.09	8.26	0.3739
2nd withdrawal	1 433 333 333	1 246 376 812	0.8696	87 / 0.05	66.8 / 0.39	0.1329	22.4	19.3	0.8616
3rd withdrawal	1 433 333 333	512 500 000	0.3576	88.6 / 0.02	25.69 / 0.90	0.0271	23.04	9.93	0.4310
4th withdrawal	1 622 727 273	228 000 000	0.1405	90 / 6.12E-17	29.46 / 0.87	7.0354E-17	23.5	11.8	0.5021
5th withdrawal	1 776 923 077	806 250 000	0.4537	90 / 6.12E-17	29.46 / 0.87	7.0354E-17	14.4	7.8	0.5417
6th withdrawal	1 611 224 490	1 007 812 500	0.6255	90 / 6.13E-17	50.9 / 0.63	9.713E-17	19.9	12.4	0.6231
7th withdrawal	1 606 153 846	215 641 791	0.1343	90 / 6.13E-17	43.1 / 0.73	8.40E-17	18.16	8.35	0.4598

Fig.28: *The sticky pollutant on the insulator surface of Kamojang switchyard*

Table 17: *The major chemical elements contained in insulator surface pollutant of Kamojang switchyard*

Chemical Elements	Compositions (%)
C	61.23
Si	11.92
Al	6.81
Cu	5.82
Fe	5.63
Ca	4.32
S	2.40
K	1.33
V	0.54

a hundred years. Based on the research and some references, a site engineer should consider that the insulators near a geothermal area or power plant have high amplitudes of leakage currents, especially if the insulators have been installing in long time and in high relative humidity, usually from night to morning. In an extreme condition, it is possible to be occurred a flashover on an insulator. It meant the insulator has been experienced a failure to serve to electrical transmission or distribution.

In a normal or low risk leakage current of insulator, the fifth harmonics of leakage current always appears. This becomes one parameter that an insulator still works in normal condition. This is experienced by most insulators on sites. Besides that, the fifth harmonics also indicates that the insulators are in capacitive condition, due to the phase angle variation which is usually followed by the fifth harmonics variation. If the phase angle reduced, which meant the power factor increased, the fifth harmonics would reduce too. For a porcelain insulator, the amplitude of fifth harmonics would decrease if the relative humidity increased. Consequently, the amplitude of fundamental harmonic would rise. Nevertheless, if this was in normal condition, the fifth harmonics was still dominant. Its amplitude was still as second highest, after the fundamental harmonics amplitude. As a comparison, this case is different from a discharge phenomenon. On the discharge condition, the most dominant harmonic after the fundamental frequency is third harmonic.

4. CONCLUSION

Based on the research results, the power factors and the leakage current amplitudes closed to humidity, and the phase angle closed to THD significantly. Otherwise, the temperature opposited to the humidity. The ratios of insulator impedance on the high and low humidity were ranged from 0.8696 until 0.1343. The small insulator impedance ratios rearched on first and seventh withdrawals. On these insulators, the THD ratios on same conditions were also small. These phenomena were caused by dry season, which amount of pollutant stuck on the insulator surfaces

significantly. On the high humidity, the phase angles became small considerably, which were between 66.8 and 25.7 degrees in these experiments. Sulphur chemical element was found in a medium composition on the pollutant. The majority of chemical elements were silicon and ferrum.

5. ACKNOWLEDGEMENTS

Authors herewith respectfully offer thanks to **THE HIGHER EDUCATION SCHOLARSHIP OF THE REPUBLIC OF INDONESIA and ASAHI GLASS FOUNDATION OF JAPAN** research projects for supporting this research.

References

[1] Fernando, M.A.R.M., Gubanski, "Performance for Non-ceramic Insulators in Tropical Environments," *PhD Dissertation, Department of Electric Power Engineering, Chalmers University of Technology*, Goteborg-Sweden, 1999, p.1-2, 70-91.

[2] E. Bacci, C. Gaggi, E. Lanzillotti, S. Ferrozzi and L. Valli, "Geothermal power plants at Mt. Amiata (Tuscany-Italy): mercury and hydrogen sulphide deposition revealed by vegetation," *Chemosphere Volume 40*, Issue 8, April 2000, P. 907-911.

[3] Dickson, M.H., Fanelli, M., " What is Geothermal Energy?," *www.geothermal-energy.org /.../ geo/ Geothermal%20Energy.en.pdf*, accessed 24th June, 2009.

[4] Eliasson, E.T., *Power Generation from High-Enthalpy Geothermal Resources*, GHC Buletin, June 2001, p.26-34.

[5] Hammons, T.J., "Geothermal Power Generation Worldwide; Global Perspective, Technology, Field Experience, and Research and Development," *Electric Power Components and Systems*, Taylor & Francis, 32, 2004, p.529-553,.

[6] Herdianita, N.R., Priadi, B., "Arsenic and Mercury Concentrations at Several Geothermal System in West Java," Indonesia, *ITB Journal Science*, Vol. 40 A, No.1, pp.1-14, 2008.

[7] Matthiasdottir, K.V., *Removal of Hydrogen Sulfide from Non-Condensable Geothermal Gas at Nesjavellir Power Plant*, www.chemeng.lth.se/exjobb/E251.pdf, accessed 24^{th} June 2009.

[8] Reed, M.J., Renner, J.L., "Alternative Fuels and the Environment," *Ch.2, Environmental Compatibility of Geothermal Energy*, ed. F.S. Sterret Boca Raton, CRC Press, 1995.

[9] Corlecci, G., Boschetti, T., Mussi, M., Lameli, C.H., Mucchino, C., Barbieri, M., "New Chemical and original isotop data on waters from El Tatio Geothermal Field," Northern Chile, *Geochemical Journal*, Vol. 39, 2005, p.547-571.

[10] Marques, J.M, Marques, J.E, Carreira, P.M., Graca, R.C., Barros, L.A., Carvalho, J.M., Chamine, H.I., Borges, F.S., "Geothermal Fluids Circulation at Caldas do Moledo Area," Northern Portugal; *geochemical and isotopic signatures*, Geofluids, 3, Blockwell Publishing, 2003, p.189-201.

[11] Markusson, S.H., Stefansson, A., Fridriksson, T., *Acid sulfate alteration of basalts in active geothermal systems*, Krísuvík, Iceland, Goldschmidt Conference Abstracts 2009, www.goldschmidt2009.org/ abstracts/ .../ A835.pdf, accessed on 24^{th} June, 2009.

[12] Gunnarsson, I., *Acid geothermal waters and elemental mobility at Krísuvík geothermal area*, www.theochem.org/ Raunvisindathing06/ .../ ig2-en.pdf, accessed on 24^{th} June, 2009.

[13] Hirowatari, K., Kusaba, S. Izumi, J., Takeuchi, K., *Production of sulfuric acid from geothermal power station exhausted gas for use in scale prevention*, em iga.igg.cnr.it/ geoworld/ pdf/ WGC/ .../ 4-Hirowatari.pdf, accessed on 24^{th} June, 2009.

[14] Loppi S, "Environmental distribution of mercury and other trace elements in the geothermal area of Bagnore (Mt. Amiata, Italy)," *Chemosphere*, Nov 2001; 45(6-7):991-5

[15] Gokcen, G., Ozturk, H.K., Hepbashi, A., *Geothermal Fields Suitable for Power Generation, Energy Source*, Taylir & Francis 26: 2004, p.441-451.

[16] Demirbas, A., *Turkey's Geothermal Energy Potential*, Energy Source, Taylor & Francis 24, 2002, p.1107-1115.

[17] Kaygusuz, K., Kaygusuz, A., *Geothermal Energy: Power for a Sustainable Future*, Energy Source, Taylor & Francis 24, 2002, p.937-947.

[18] EcoLogoCm Program Management, (D) Geothermal-Powered Electricity; CCD-003: Electricity-Renewable Low-Impact, EcoLogoCM Program Criteria Review, Certification Discussion Document, 2008, p.8-13.

[19] Otsubo, M., Hashiguchi, T., Honda, C., "Evaluation of Insulation Performance of Polymeric Surface using a Novel Separation Technique of Leakage Current," *IEEE Transactions on Dielectrics and Electrical Insulation*, Vol. 10, No.6, December 2003.

[20] Farzaneh, M., Fofana, I., "Study of Insulator Flashovers caused by Atmospheric Ice Accumulation," *Journal of Iranian Association of Electrical and Electronics Engineers*, Vol.1, No.1, Spring 2004.

[21] Reddy, B.S., Nagabhushana, G.R., "Study of Leakage Current Behaviour on Artificially Polluted Surface of Ceramic Insulator," *Plasma Science and Technology*, Vo.5, No.4 (2003).

[22] Fofana, I., Tavakoli, C., Farzaneh, M., "Dynamic

Modelling of AC Iced Insulator Flashover Characteristics," *Paper accepted for presentation at 2003 IEEE Bologna Power Technology Conference*, June 23-26th, 2003, Bologna, Italy.

[23] El-Hag, A.H., Jayaram, S.H., Cherney, E.A., "Fundamental and Low Frequency Harmonic Components of Leakage Current as a Diagnostic Tool to Study Aging of RTV and HTV Silicone Rubber in Salt-Fog," *IEEE Transactions on Dielectrics and Electrical insulation*, Vol.10, No.1, February 2003.

[24] Devendranath, D., Channakeshava, "Leakage Current and Charge in RTV Coated Insulators Under Pollution Conditions," *IEEE Transactions on Dielectrics and Electrical insulation*, Vo. 9, No.2, April 2002.

[25] Moreno, V.M., Gorur, R.S., "Effect of Long-term Corona on Non-ceramic Outdoor Insulator Housing Materials," *IEEE Transactions on Dielectrics and Electrical insulation*, Vol.8, No.1, February 2001.

[26] Dixit, P., Gopal, H.G., Letter to the Editor: Variation of Leakage Current with SDD on an Artificially Polluted Porcelain Pin Insulator - AN Experimental Study, Electrical Power Components and Systems, 35, p.359-365, 2007.

[27] Jiang, X., Wang, S., Zhang, Z., Xie, S., Wang, Y., "Study on AC Flashover Performance and Discharge Process of Polluted and Iced IEC Standard Suspension Insulator String," *Proceedings of the XIVth International Symposium on High Voltage Engineering*, Tsinghua University, Beijing, China, August 25-29, 2005.

[28] Sun, C., Jiang, X., Shu, L., Lu, Z., Chen, M., "AC Flashover Performance and Mechanism of Polluted and Iced IEC Standard Suspension Insulator String," *Proceeding of The Thriteenth (2003) International Offshore and Polar Engineering Conference*, Honolulu, Hawaii, USA, May 25-30, 2003.

[29] Awad, M.M., Said, H.M., Arafa, B.A., Sadeek, A.E.H., *Effect of Sandstorms with Charged Particles on The Flashover and Breakdown of Transmission Lines*, Cigre, Sessin 2002, 15-306.

[30] Zegnini, B., Mahi, D., Vega, J.M., "Modeling AC Arcs Developing along Electrolytic Surfaces Simulating Practical Polluted Insulator Using an Original Laboratory Model," *International Journal of Applied Engineering Research*, Vol.2, No.1, 2007, p.109-124.

[31] Vosloo, W. L., Holthhausen, "A Comparison of the Performance of High-Voltage Insulator Materials in a Severely Polluted Coastal Environment," *PhD Dissertation, Department of Electrical and Electronic Engineering*, University of Stellenbosch, South Africa, March 2002, p.118-150.

[32] OriginLab Co., *Origin V75 User's Manual, OriginLab Corporation*, MA,USA, pp.601-611, 2003.

[33] Suwarno, "Leakage Current Waveforms of Outdoor Polymeric Insulators and Possibility of Application for Diagnostics of Insulator Conditions," *Journal of Electrical Engineering & Technology, The Korean Institute of Electrical Engineering*, Vol.1,No.1,pp.114-119, 2006.

[34] Anderson, *T.W. An Introduction to Multivariate Statistical Analysis*, Second Edition, John Wiley & Sons, pp.18,489, 1984.

[35] Whittaker, J., *Graphical Models in Applied Multivariate Statistics*, John Wiley & Sons, pp.17,48-51, 1996.

[36] Hannawati A., Thiang, Prasetyo Y., "Odor Recognition dengan Menggunakan Principal Component Analysis dan Nearest Neighbour Classifier," *http:// puslit.petra.ac.id/ journals/ electrical*, accessed on 1st Dec. 2007.

[37] Mardia, K.V., Kent, J.T., Bibby, J.M., *Multivariate Analysis*, Academic Press, London, UK, pp.213-228, 2000.

[38] Lab. Perencanaan dan Optimasi Sistem Industri, "Handout multivariate Analysis," *Seminar and Workshop*, Teknik Industri ITB, 17th & 24th March, 2007.

Waluyo was born in Magelang, Central Java, Indonesia, in 1969. He is presently a doctoral student at School of Electrical Engineering and Informatics, Bandung Institute of Technology (ITB) and an associate professor lecturer at National Institute of Technology Bandung, Indonesia. His bachelor and master degrees were from ITB too. He is interested in high voltage engineering.

Ngapuli Irmea Sinisuka was born in Indonesia, in 1950. He is presently a full professor senior lecturer at School of Electrical Engineering and Informatics, ITB, Indonesia. He is interested in electrical high voltage materials. His bachelor was from ITB, master and doctorate degrees were from Electronique, Institute National Polytechnique De Grenoble, France and Electronique, Electrotechnique, Automatique, Universite Paul Sabatier-Toulouse III, France respectively

Suwarno was born in Indonesia, in 1965. He is presently an associate professor lecturer at School of Electrical Engineering and Informatics, ITB, Indonesia and member of IEEE. His bachelor and master degrees were from ITB, and his Doctorate was from Nagoya University, Japan. He is interested in electrical high voltage materials.

Maman Abdurahman Djauhari was born in Indonesia, in 1949. He is presently a full professor senior lecturer at Department of Mathematics, ITB, Indonesia. He is interested in multivariate and robust statistics. His bachelor was from ITB, and his Master and Doctorate degrees were from Universite de Montpellier, France.